A Cre-loxP-based mouse model for conditional somatic gene expression and knockdown *in vivo* by using avian retroviral vectors

Barbara Seidler, Annegret Schmidt, Ulrich Mayr, Hassan Nakhai, Roland M. Schmid, Günter Schneider, and Dieter Saur*

Department of Internal Medicine 2, Technische Universität München, Ismaningerstrasse 22, 81675 Munich, Germany

Edited by Peter K. Vogt, The Scripps Research Institute, La Jolla, CA, and approved April 17, 2008 (received for review January 16, 2008)

Site- and time-specific somatic gene transfer by using the avian sarcoma-leukosis retrovirus RCAS (replication-competent avian sarcoma-leukosis virus long terminal repeat with splice acceptor) has been shown to be a powerful tool to analyze gene function *in vivo*. RCAS retroviruses that express the avian subgroup A envelope transduce only mammalian cells genetically engineered to express the avian retroviral receptor, tumor virus A (TVA). Here, we generated a knockin mouse line termed *LSL-R26*$^{Tva\text{-}lacZ}$ with concomitant conditional expression of TVA and lacZ by targeting the *Rosa26* locus. A loxP-flanked transcriptional stop cassette was used for conditional activation of TVA and LacZ expression in a Cre-recombinase-dependent manner. To demonstrate the ability of this system for conditional somatic gene transfer *in vivo*, we directed TVA expression to the pancreas. Introduction of an RCAS vector with Bryan-RSV polymerase and subgroup A envelope [RCASBP(A)] carrying oncogenic *Kras*^{G12D} induced focal ductal pancreatic lesions that recapitulate human pancreatic intraepithelial neoplasias that progress to pancreatic ductal adenocarcinomas. TVA-mediated infection of genetically engineered mice with endogenous expression of Kras^{G12D} in pancreatic progenitor cells by using RCASBP(A) virus carrying a short hairpin RNA directed against murine TP53, resulted in dramatically enhanced progression to invasive adenocarcinomas. These results show that conditional expression of TVA enables spatiotemporal gene expression and knockdown in a small subset of somatic cells *in vivo*. Therefore, it closely models carcinogenesis in humans where tumors evolve from somatic gene mutations in developmentally normal cells. Combined with the growing number of Cre expression models, RCAS-TVA-based gene expression and knockdown systems open up promising perspectives for analysis of gene function in a time-controlled and tissue-specific fashion *in vitro* and *in vivo*.

pancreatic cancer | RCAS | tumor virus A | RNA interference | molecular *in vivo* imaging

In the postgenome area, there is an increasing need for tools allowing the spatiotemporal evaluation of gene function *in vivo*. Genetically engineered mouse models that permit conditional expression or inactivation of genes have dramatically improved our basic understanding of gene function *in vivo*. However, gene knockout and knockin technologies such as the Cre-loxP system are difficult, time-consuming, and expensive (1). This problem can be overcome with an alternative strategy by using avian retroviral vectors to deliver genes to specific proliferating somatic mammalian cells (2–4). The retroviral RCASBP(A) (replication competent avian sarcoma-leukosis virus long terminal repeat with splice acceptor, Bryan RSV polymerase and subgroup A envelope)-expression vector derived from subgroup A avian sarcoma-leukosis virus can be used to produce high-titer viral stocks in chicken DF-1 fibroblasts and deliver transgenes stable to proliferating cells that express the specific receptor for avian sarcoma-leukosis virus subgroup A envelope (envA), tumor virus A (TVA) (2, 5, 6). In addition, other retroviral or lentiviral vectors can be pseudotyped with envA and used to transduce TVA-positive cells (7). Mammalian cells do not express TVA and therefore are resistant to infection by RCASBP(A) viruses. However, ectopic expression of TVA confers susceptibility to infection *in vitro* and *in vivo*. Because RCASBP(A) viruses are replication incompetent in mammalian cells, the virus does not spread (2–4). The RCASBP(A) vector itself does not cause a significant immune response in the host (8). However, an immune response against foreign genes expressed by RCAS-mediated gene transfer has been observed. Interestingly, the extent of the immune response seems to be tissue specific, which may limit the use of the RCAS-TVA system in certain tissue types (8). Mammalian cells remain susceptible to reinfection, which allows simultaneous or sequential introduction of genes into the same cells. This makes the system particularly useful to study the cooperation of specific genes (3, 9).

The RCAS-TVA somatic gene transfer system has been used in a variety of murine models *in vivo* (9–19), and the advantages and disadvantages are well documented (2–4). In particular, the system has been widely used to model sporadic human cancer in mice. For example, glioblastoma, ovary cancer, pancreatic cancer, liver cancer, and mammary cancer have been induced by the introduction of oncogenes in a tissue-specific fashion (9, 12, 15, 17, 18). Interestingly, all existing TVA-expressing mouse lines have been generated by random transgenesis by using pronuclear injection that often results in variable and mosaic transgene expression. Cell-specific TVA expression has been achieved in these models by using tissue-specific promoters. Therefore, individual transgenic lines must be generated for different tissue types that limit the broad use of the system.

To generate a universal, tissue-specific RCAS-TVA retroviral gene delivery model, we have established Cre-loxP-based conditional TVA expression by targeting the *Rosa26* locus in mice. We show that conditional TVA expression allows for transgene expression and for RNA interference (RNAi) in a tissue-specific and time-controlled fashion *in vivo*. Transduction of pancreatic progenitor cells with activated oncogenic Kras^{G12D} induces mouse pancreatic intraepithelial neoplasia (mPanIN) that progress to invasive pancreatic ductal adenocarcinomas (PDACs). RCASPB(A)-based knockdown of TP53 by RNAi in mice with pancreas-specific endogenous expression of Kras^{G12D} resulted in a dramatically increased acceleration of PDAC formation. Therefore, our RCAS-TVA-based mouse model adds a powerful tool to analyze gene function and collaborative

Author contributions: B.S. and A.S. contributed equally to this work; B.S., R.M.S., G.S., and D.S. designed research; B.S., A.S., U.M., and D.S. performed research; H.N. and R.M.S. contributed new reagents/analytic tools; B.S., A.S., U.M., and D.S. analyzed data; and B.S., G.S., and D.S. wrote the paper.

The authors declare no conflict of interest.

This article is a PNAS Direct Submission.

*To whom correspondence should be addressed. E-mail: dieter.saur@lrz.tum.de.

This article contains supporting information online at www.pnas.org/cgi/content/full/0800487105/DCSupplemental.

genetic interactions in a broad range of tissue types *in vivo* by taking advantage of the Cre-loxP recombination strategy.

Results and Discussion

Conditional Cre-Regulated TVA Expression *in Vitro*. As a first step toward generating a conditional *TVA* transgenic mouse line, we tested different approaches to ensure that TVA is expressed only after Cre-mediated recombination. As shown in supporting information (SI) Fig. S1, insertion of an optimized loxP-flanked stop element (lox-stop-lox; LSL) 5′ of the *firefly luciferase* (*fLuc*) gene resulted in efficient blockade of fLuc expression from the strong *CMV* promoter. However, when we tested this LSL element by using a plasmid termed pRosa26-LSL-ATG-TVA (see Fig. S2*A*), which comprises the *Rosa26* promoter, the LSL cassette, the *TVA* coding sequence, an internal ribosome entry site (IRES), and a *lacZ* expression cassette with a nuclear localization signal (*lacZnls*), transiently transfected cells remained susceptible to RCAS-mediated retroviral transduction (Fig. S2 *B* and *D*). This observation indicates unwanted transcriptional read-through into the *TVA* coding sequence and low abundant TVA expression in the absence of Cre-mediated excision of the floxed stop cassette. Therefore, we subsequently disrupted the *TVA* transgene just after the ATG start codon by the LSL cassette (ATG-LSL-Tva; Fig. S2*A*). Consequently, any transcriptional read-through followed by translational initiation downstream of the LSL element would generate a truncated and putative inactive TVA receptor. As expected, this construct reliably prevented expression of functional TVA and rendered transfected mammalian cells resistant to RCASBP(A)-mediated retroviral gene transfer, as demonstrated by luciferase assays and testing for alkaline phosphatase (AP) activity after infection with RCASBP(A)-fLuc or RCASBP(A)-AP, respectively (Fig. S2 *B* and *F*). To prove functionality of the altered TVA receptor, which is mutated at the N-terminal end because of the insertion of one loxP site after Cre-mediated recombination (see Fig. S2*A*), we cotransfected pRosa26-LSL-ATG-Tva and pRosa26-ATG-LSL-Tva plasmids with a Cre-recombinase expression plasmid (pIC-Cre), respectively. Subsequently, we transduced cells with RCASBP(A)-fLuc. As shown in Fig. S2*B*, expression of the mutated TVA receptor resulted in a similar fLuc activity compared with cells expressing the wild-type receptor. This indicates that mutation of the TVA receptor at the N-terminal end does not diminish retroviral infection.

Conditional Cre-Regulated TVA and LacZnls Expression *in Vivo*. To create a conditional mouse line that is capable of TVA expression in any cell type after Cre-recombinase-mediated excision of the LSL element, which disrupts and silences the *TVA* transgene, we have targeted the broadly expressed *Rosa26* (*R26*) locus by homologous recombination in embryonic stem (ES) cells (20). We refer to this strain as *LSL-R26*$^{Tva\text{-}lacZ}$. To generate *LSL-R26*$^{Tva\text{-}lacZ}$ mice, we electroporated a pRosa26-ATG-LSL-Tva-IRES-lacZnls targeting vector (Fig. S3*A*) into 129S6 ES cells. By using PCR and Southern blot analyses, we observed that 36 of 192 geneticin-resistant colonies had correctly undergone homologous recombination (Fig. S3*B*). We used clones 1 and 4 to derive germ-line chimeras, which we then bred with C57BL/6J females to obtain heterozygous *LSL-R26*$^{Tva\text{-}lacZ}$ progeny on a mixed 129S6;C57BL/6J genetic background (Fig. S3*C*). Both heterozygous and homozygous *LSL-R26*$^{Tva\text{-}lacZ}$ mice did not show any phenotype and are viable and fertile with normal lifespan. We assessed Cre-dependent TVA and lacZnls expression in embryos and postnatal animals obtained from matings between heterozygous *LSL-R26*$^{Tva\text{-}lacZ}$ mice and *protamin-Cre* (*Prm-Cre*) transgenic mice, the latter being a general deleter strain in which Cre is expressed from the *protamin* promoter (21). By using β-galactosidase staining, we observed ubiquitous lacZnls expression in *LSL-R26*$^{Tva\text{-}lacZ/+}$*;Prm-Cre* embryos and adult tissues but did not detect lacZ activity in singly transgenic animals (Fig. 1 *A–C* and *H* and data not shown). By using quantitative real-time RT-PCR, we obtained similar results for TVA mRNA expression (Fig. S4). These results indicate that TVA and lacZnls expression is strictly dependent on Cre-mediated excision of the LSL cassette. After recombination, TVA and lacZnls are expressed in all cells throughout embryogenesis and in adulthood under the control of the *Rosa26* promoter. This is consistent with previous studies in which the *Rosa26* promoter was found to be activated from preimplantation onward (20). To prove tissue-specific expression of TVA and lacZnls, we crossed *LSL-R26*$^{Tva\text{-}lacZ/+}$ mice with *Ptf1a/p48*$^{Cre/+}$ animals, a knockin mouse line where Cre expression is restricted to the pancreas and neurons of the retina, cerebellum, and dorsal neural tube (22). Cre-mediated recombination of the LSL element in the pancreas, but not other abdominal organs, was verified by Southern blot analysis of *Ptf1a/p48*$^{Cre/+}$*;LSL-R26*$^{Tva\text{-}lacZ/+}$ mice (Fig. S3*D*). As expected, we observed that LacZnls (Fig. 1 *D–G*) and TVA (Fig. 1 *I* and *J*) expression was restricted to the pancreas in these mice, as demonstrated by X-Gal staining and immunohistochemistry by using a polyclonal TVA-specific antibody, respectively. In line, high amounts of TVA mRNA are expressed in the pancreas of *LSL-R26*$^{Tva\text{-}lacZ/+}$*;Ptf1a/p48*$^{Cre/+}$ animals, whereas only trace amounts are present in other organs (Fig. S4). To test whether the *Rosa26* locus is also active in mPanIN lesions and PDAC of mice with endogenous expression of oncogenic Kras^{G12D} (23) or concomitant expression of Kras^{G12D} and mutant TP53^{R172H} (24), we crossed *LSL-R26*$^{Tva\text{-}lacZ/+}$ mice with *Ptf1a/p48*$^{Cre/+}$*;LSL-Kras*$^{G12D/+}$ and *Ptf1a/p48*$^{Cre/+}$*;LSL-Kras*$^{G12D/+}$;TP53^{+} animals, respectively. As shown in Fig. 1, we found strong X-Gal staining and TVA immunoreactivity in mPanINs (*M* and *N*), primary PDAC (*O* and *P*), and the corresponding liver metastases (*Q*), but not in desmoplastic stroma.

RCASBP(A)-Mediated Retroviral Gene Transfer *in Vitro* and *in Vivo*. To prove the principle that RCASBP(A)-mediated retroviral transduction can be achieved in a spatially and temporally controlled fashion, we first crossed *LSL-R26*$^{Tva\text{-}lacZ/+}$ and *Prm-Cre* mice and isolated primary murine embryonal fibroblasts (MEFs) from compound heterozygous and singly transgenic mice. To show that *LSL-R26*$^{Tva\text{-}lacZ/+}$*;Prm-Cre* but not *LSL-R26*$^{Tva\text{-}lacZ}$ MEFs are susceptible to infection with RCASBP(A) viruses, we transduced them with high titers (10^8 units/ml) of RCASBP(A)-EGFP, which carries an expression cassette for enhanced green fluorescent protein (EGFP). Three days later, we observed strong EGFP expression of *LSL-R26*$^{Tva\text{-}lacZ/+}$*;Prm-Cre* MEFs, but not *LSL-R26*$^{Tva\text{-}lacZ/+}$ MEFs, indicating that the LSL element reliably prevents functional expression of the TVA receptor (Fig. S5).

To test whether conditional retroviral transduction can be achieved *in vivo*, we injected different amounts (1×10^6 and 5×10^7) of DF-1 cells that produce high titers of RCASBP(A)-EGFP i.p into *LSL-R26*$^{Tva\text{-}lacZ/+}$*;Ptf1a/p48*$^{Cre/+}$ animals. Because cell proliferation is necessary for effective RCAS-mediated retroviral transduction (2, 3, 19), 2-day-old animals were used as described by Lewis *et al.* (15). Three weeks later, we found strong and reliable EGFP expression in a small number (<1%) of cells in pancreatic cryosections of animals injected with 5×10^7 (Fig. 2 *A* and *B*) but not 1×10^6 DF-1 cells. Other gastrointestinal organs showed no EGFP expression (data not shown). Of note, no immune response was observed in animals injected with DF-1 cells. Control animals (*LSL-R26*$^{Tva\text{-}lacZ/+}$ and *Ptf1a/p48*$^{Cre/+}$) infected with RCASBP(A)-EGFP showed no EGFP expression in any organ of the gastrointestinal tract (data not shown). To prove that proliferating mPanIN lesions and PDAC are susceptible to RCASBP(A) infection *in vivo*, we subsequently injected 10^7 DF-1 RCASBP(A)-EGFP cells othotopically into the pan-

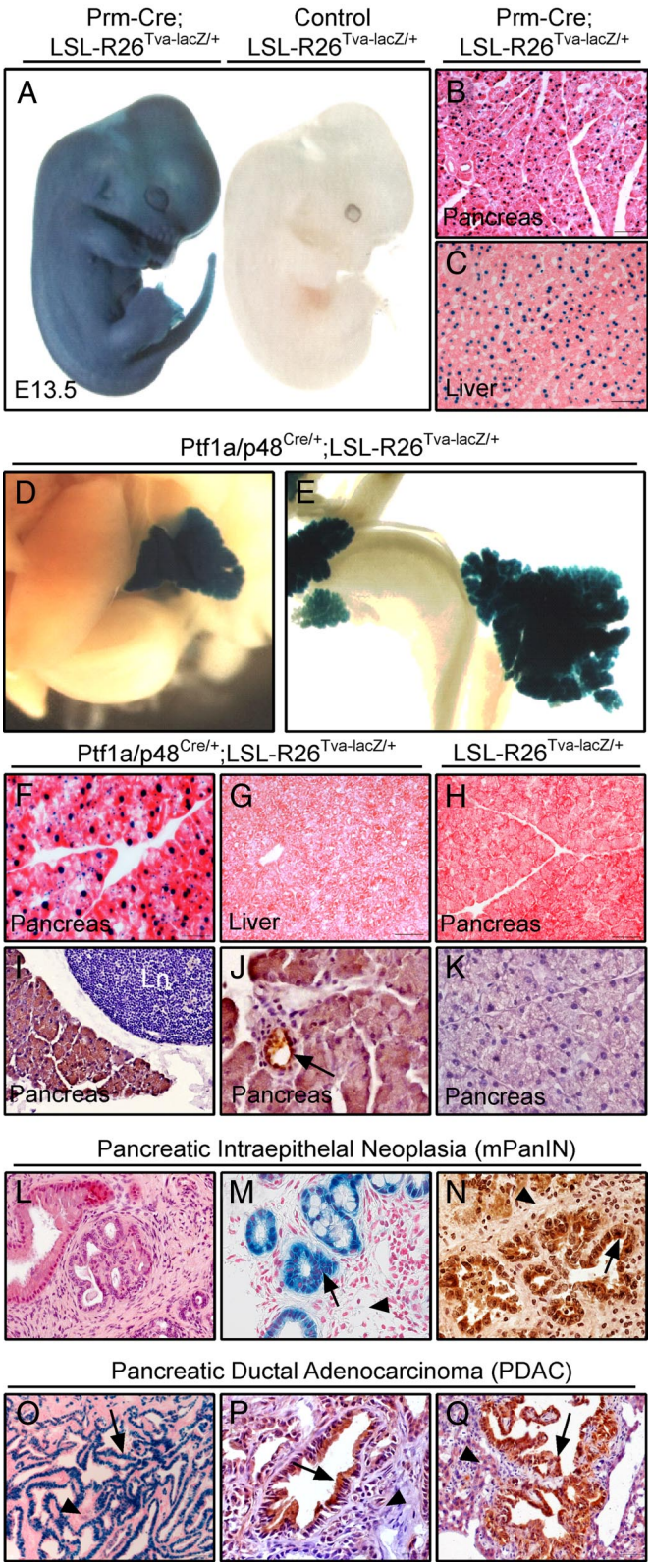

Fig. 1. Characterization of *LSL-R26*$^{Tva\text{-}lacZ}$ knockin mice. (*A*) Whole-mount X-Gal staining of E13.5 *LSL-R26*$^{Tva\text{-}lacZ/+}$*;Prm-Cre* (*Left*) and *LSL-R26*$^{Tva\text{-}lacZ/+}$ (*Right*) embryos. (*B* and *C*) Nuclear lacZ activity in sections of the pancreas (*B*) and liver (*C*) isolated from adult *LSL-R26*$^{Tva\text{-}lacZ/+}$*;Prm-Cre* mouse. (*D–G*) Visualization of lacZ activity in *LSL-R26*$^{Tva\text{-}lacZ/+}$*;Ptf1a/p48*$^{Cre/+}$ mice. Macroscopic images of X-Gal-stained liver and pancreas (*D*) and small bowel and pancreas (*E*) of E18 embryo. Microscopic images of nuclear lacZ activity in sections of the pancreas (*F*) and the liver (*G*) of adult mouse. (*H*) X-Gal staining reveals no lacZ activity in pancreatic sections of adult *LSL-R26*$^{Tva\text{-}lacZ/+}$ mouse (control). (*I–K*) Immunostaining for TVA (brown color) in the pancreas of adult *LSL-R26*$^{Tva\text{-}lacZ/+}$*;Ptf1a/p48*$^{Cre/+}$ (*I* and *J*) and control *LSL-R26*$^{Tva\text{-}lacZ/+}$ (*K*) mouse. TVA is expressed in islets (data not shown), ducts (black arrow in *J*) and acini (*I* and *J*), but not adjacent lymph node (Ln in *I*). (*L–N*) Expression of lacZnls and TVA in mPanIN lesions of *Ptf1a/p48*$^{Cre/+}$*;LSL-R26*$^{Tva\text{-}lacZ/+}$*;LSL-Kras*$^{G12D/+}$ animals. Hematoxylin and eosin (H&E) (*L*), X-Gal (*M*) and immunohistochemical TVA (*N*) staining of pancreatic sections showing expression of nuclear lacZ (*M*) and TVA (*N*) in mPanIN lesions (black arrows) but not desmoplastic stroma (black arrowheads). (*O–Q*) Expression of TVA and lacZnls in murine PDAC of *Ptf1a/p48*$^{Cre/+}$*;LSL-R26*$^{Tva\text{-}lacZ/+}$*;LSL-Kras*$^{G12D/+}$*;LSL-TP53*$^{R172H/+}$ animals. X-Gal (*O*) and immunohistochemical TVA (*P* and *Q*) staining of sections from primary PDAC (*O* and *P*) and liver metastases (*Q*) showing expression of nuclear lacZ and TVA in PDAC (black arrow) but not desmoplastic stroma (*O* and *P*; black arrowheads) or adjacent normal liver (*Q*; black arrowhead).

creas of 3-week-old *LSL-R26*$^{Tva\text{-}lacZ/+}$*;Ptf1a/p48*$^{Cre/+}$*;LSL-Kras*$^{G12D/+}$ or 16-week-old *LSL-R26*$^{Tva\text{-}lacZ/+}$*;Ptf1a/p48*$^{Cre/+}$*;LSL-Kras*$^{G12D/+}$;TP53^{+} compound mutant mice, respectively. As shown in Fig. 2, we observed EGFP-positive acini (*C* and *D*), mPanIN lesions (*C–F*), primary PDAC (*G*, *H*, *J*, *K*, *M*, and *N*), and liver metastases (*I* and *L*). We therefore conclude that TVA expression renders proliferating normal, preneoplastic, and neoplastic cells susceptible to RCASBP(A) virus infection *in vivo*.

Introduction of *Kras*^{G12D} into Ptf1a/p48-Positive Cells Induce mPanIN Lesions and PDAC. Activating mutations in the *Kras* proto-oncogene are found in >90% of human PDAC and therefore, are supposed to represent an initiating carcinogenic event (25, 26). In line, endogenous expression of oncogenic Kras^{G12D} at physiological levels in the murine pancreas induces mPanIN lesions and metastatic PDAC (see Fig. 1 *L–Q*) (23, 27). To determine the effects of retroviral delivered oncogenic *Kras*^{G12D}, we transduced proliferating cells in the pancreas of *LSL-R26*$^{Tva\text{-}lacZ/+}$*;Ptf1a/p48*$^{Cre/+}$ mice with RCASBP(A)-Kras^{G12D} 2 days after birth (P2; Fig. 3*A*). Nine months after infection, RCASBP(A)-Kras^{G12D}- but not RCASBP(A)-EGFP-infected compound mutant mice developed focal ductal pancreatic lesions with incomplete penetrance (4 of 5 animals). These lesions closely resembled human PanINs and were indistinguishable from mPanINs of mice with endogenous expression of Kras^{G12D} (Fig. 3 *B–D*) (23). They met the criteria of mouse PanIN lesions described by a recent consensus report (28). We next analyzed PDAC development in a cohort of five *LSL-R26*$^{Tva\text{-}lacZ/+}$*;Ptf1a/p48*$^{Cre/+}$ mice infected with RCASBP(A)-Kras^{G12D} or RCASBP(A)-EGFP. Three of five mice infected with RCASBP(A)-Kras^{G12D} but none of the RCASBP(A)-EGFP-infected littermates developed invasive and metastatic PDAC after 19 months (Fig. 3 *E–J*). All PDAC displayed a ductal phenotype, an intense desmoplastic stroma, and local infiltration (Fig. 3 *G–J*) closely resembling the human disease and similar to those observed in mice with endogenous expression of Kras^{G12D} in Ptf1a/p48-positive pancreatic progenitor cells from embryonic day 9.5 onward (23, 24). Furthermore, all PDACs were CK19-positive (Fig. 3*J*) and two mice developed liver and lymph node metastases (Fig. 3 *F* and *I* and data not shown). To verify that PDACs develop because of infection with Kras^{G12D}, we amplified cDNA isolated from primary PDAC by PCR using Kras-specific primers. Sequencing of the PCR products revealed expression of mutant Kras^{G12D} mRNA in the tumors. In contrast, only wild-type Kras was present in all other abdominal organs (data not shown). In addition, we confirmed presence of RCASBP(A) proviral DNA in tumors from mice infected with RCASBP(A)-Kras^{G12D} by PCR (Fig. S6*A*). Restriction mapping by Southern blot analysis with a probe directed against the RCASBP(A) *envA* gene revealed that PDACs induced by RCASBP(A)-Kras^{G12D} have single or multiple provirus integration sites (Fig. S6*B*). This indicates that retroviral infection of the

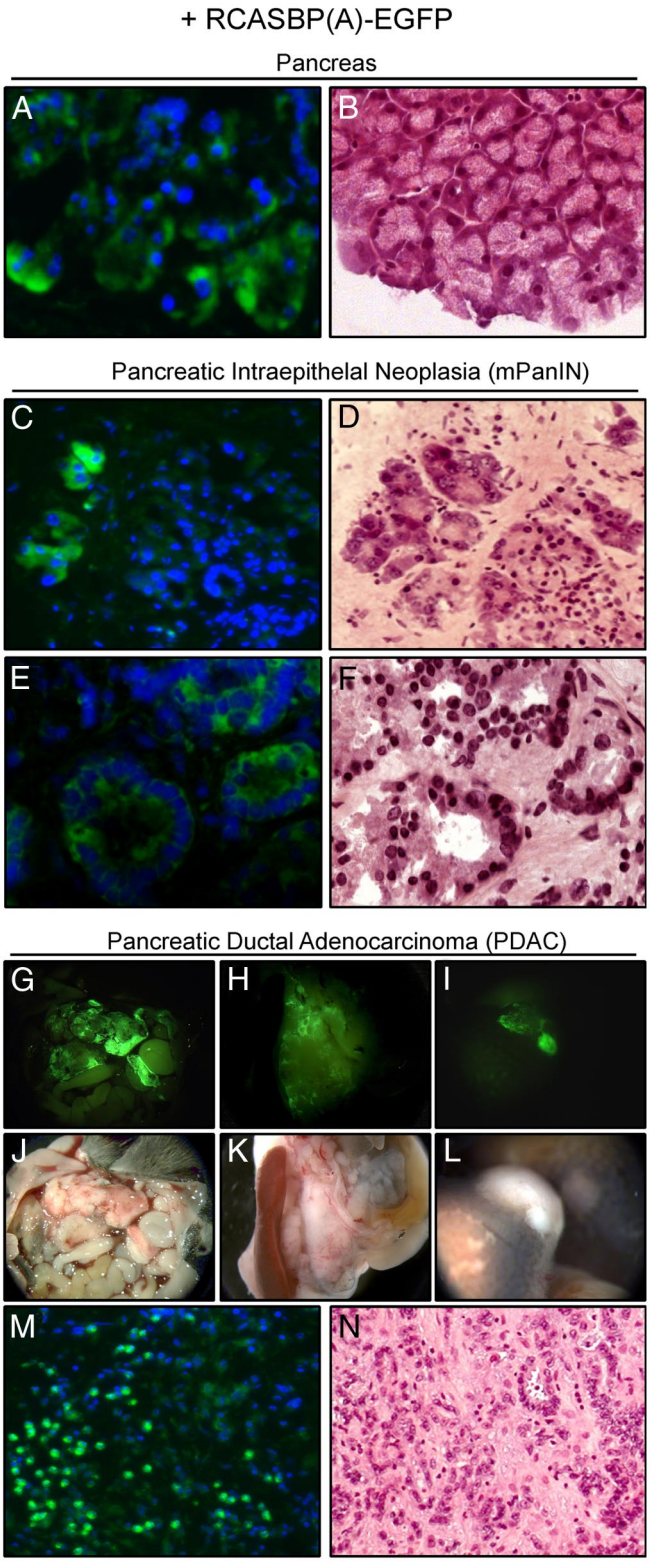

Fig. 2. Ectopic expression of TVA renders murine cells susceptible to retroviral RCASBP(A)-mediated somatic gene transfer *in vivo*. (*A–N*) Retroviral transduction of the pancreas, mPanIN lesions, and PDAC *in vivo*. Mice were infected by injection of DF-1 RCASBP(A)-EGFP cells as described in *Materials and Methods*. Serial cryosections of the pancreas of *Ptf1a/p48*$^{Cre/+}$;*LSL-R26*$^{Tva\text{-}lacZ/+}$ (*A* and *B*) and *Ptf1a/p48*$^{Cre/+}$;*LSL-R26*$^{Tva\text{-}lacZ/+}$;*LSL-Kras*$^{G12D/+}$ (*C–F*) animals were DAPI (*A, C,* and *E*) or H&E (*B, D,* and *F*) stained and subjected to fluorescence (*A*, *C,* and *E*) and white-light (*B*, *D*, and *F*) imaging. (*G–L*) Macroscopic view of RCASBP(A)-EGFP-infected *Ptf1a/p48*$^{Cre/+}$;*LSL-R26*$^{Tva\text{-}lacZ/+}$;*LSL-Kras*$^{G12D/+}$;*LSL-TP53*$^{R172H/+}$ mouse with metastatic PDAC. EGFP expression of PDAC was visualized by fluorescence stereomicroscopy. Fluorescent (*G–I*) and corresponding white-light (*J–L*) images of primary PDAC (*G*, *H*, *J*, and *K*) and liver metastases (*I* and *L*). (*M* and *N*) Microscopic fluorescent (*M*) and white-light (*N*) images of DAPI (*M*) and H&E (*N*) stained serial cryosections of primary PDAC of RCASBP(A)-EGFP-infected *Ptf1a/p48*$^{Cre/+}$;*LSL-R26*$^{Tva\text{-}lacZ/+}$;*LSL-Kras*$^{G12D/+}$;*LSL-TP53*$^{R172H/+}$ mouse.

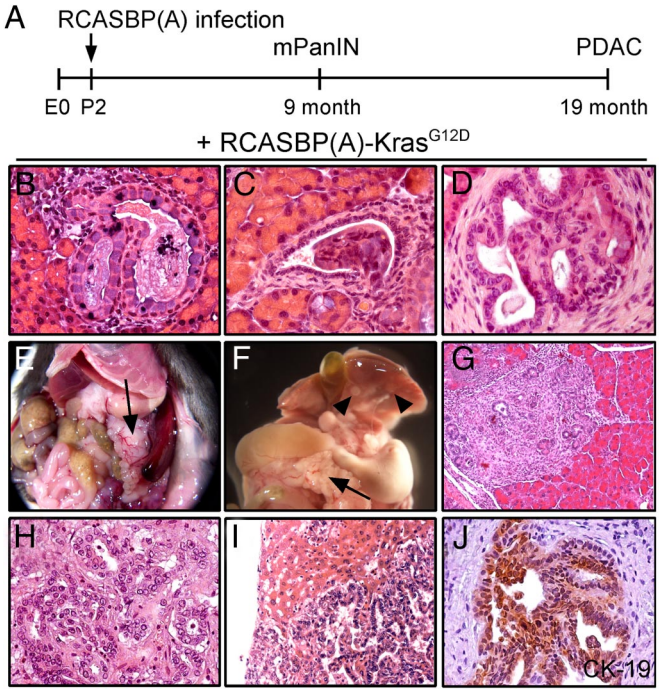

Fig. 3. Retroviral RCASBP(A)-Kras^{G12D} infection induces mPanIN lesions and PDAC in *Ptf1a/p48*$^{Cre/+}$;*LSL-R26*$^{Tva\text{-}lacZ/+}$ mice. (*A*) Two-day-old mice (P2) were infected with RCASBP(A)-Kras^{G12D} or RCASBP(A)-EGFP as control as described in *Materials and Methods*. Mice were analyzed at the indicated time points. Development of mPanIN and PDAC in RCASBP(A)-Kras^{G12D}-infected animals is indicated. (*B–D*) H&E-stained pancreatic paraffin sections of *Ptf1a/p48*$^{Cre/+}$;*LSL-R26*$^{Tva\text{-}lacZ/+}$ mice 9 months after infection with RCASBP(A)-Kras^{G12D} showing focal ductal lesions resembling mPanIN1A (*B*) and mPanIN2 (*C* and *D*). (*E* and *F*) Macroscopic view of PDAC arising in 19-month-old RCASBP(A)-Kras^{G12D}-infected mice. Black arrow indicates nodular pancreas (*E* and *F*). Liver metastases are indicated by black arrowheads (*F*). (*G–I*) H&E stain of early stage (*G*) and advanced PDAC (*H*), and liver metastase (*I*) arising in *Ptf1a/p48*$^{Cre/+}$;*LSL-R26*$^{Tva\text{-}lacZ/+}$ mice after infection with RCASBP(A)-Kras^{G12D}. (*J*) CK-19 immunohistochemistry shows intense staining in well differentiated primary PDAC.

pancreas with RCASBP(A)-Kras^{G12D} results in monoclonal tumors (PDAC 1 in Fig. S6*B*) and most likely oligoclonal tumors (PDACs 2 and 3 in Fig. S6*B*) that arise from independently infected cells with a single provirus integration. This is consistent with a recent report showing that RCASBP(A)-PyMT induced oligoclonal mammary tumors (18). However, because of the injection of a very large number of DF-1 cells (5×10^7) it is also possible that PDACs 2 and 3 are monoclonal tumors that arose from multiple provirus integrations into the same cell.

Conditional Down-Regulation of TP53 *in Vivo* Accelerates Tumor Formation in Mice with Endogenous Expression of Oncogenic Kras^{G12D} in Progenitor Cells of the Pancreas. To study the cooperation of oncogenes and tumor suppressor genes for initiation and progression of PDAC, we evaluated the RCAS-TVA system for knockdown of tumor suppressor genes by RNAi in a spatially and temporally controlled manner. To test whether RCAS-induced RNAi is feasible *in vivo*, we first evaluated gene knockdown of fLuc in MiaPaCa2$^{fLuc\text{-}IRES\text{-}TVA}$ pancreatic cancer cells with sta-

ble concomitant expression of fLuc and TVA. We transplanted these cells orthotopically into the pancreas of nude mice and subsequently transduced them with RCASBP(A) virus carrying a shRNA against fLuc under the control of the human *H1* promoter (RCASBP(A)-shfLuc). Longitudinal *in vivo* bioluminescence imaging revealed efficient knockdown of fLuc expression in tumor-bearing mice after infection with RCASBP(A)-shfLuc compared with tumors transduced with a control shRNA (RCASBP(A)-shControl) (Fig. S7). Therefore, RCAS-mediated gene silencing is feasible not only *in vitro* (29), but also *in vivo* in mice. To date RCAS-mediated RNAi *in vivo* has been shown only in chicken (30).

After demonstrating that delivery of shRNAs by RCASBP(A) viruses results in a profound knockdown of gene expression *in vivo*, we subsequently used the aforementioned PDAC model (*Ptf1a/p48$^{Cre/+}$;LSL-Kras$^{G12D/+}$*) in which oncogenic Kras^{G12D} is expressed from its endogenous promoter in Ptf1a/p48-positive pancreatic progenitor cells (23). These mice develop mPanIN lesions as early as 2 weeks after birth that progress to invasive PDACs with a median latency of 14 months. To assess the cooperation of oncogenic *Kras^{G12D}* with loss or inactivation of the tumor supressor gene *TP53*, we infected 3-week-old mice with RCASBP(A) vectors expressing a shRNA against murine TP53 (31). *Ptf1a/p48$^{Cre/+}$;LSL-R26$^{Tva-lacZ/+}$;LSL-Kras$^{G12D/+}$* animals infected with RCASBP(A)-shTP53 have a dramatically, statistically significant shortened latency of PDAC development with a median survival of ≈5 months compared with RCASBP(A)-shControl-infected littermates (P = 0,0064, log-rank test; Fig. 4*A*). Of note, all RCASBP(A)-shTP53-infected animals developed invasive PDAC within 10 months (Fig. 4 *B–G*) indicating that RCAS-mediated silencing of TP53 resulted in a dramatically enhanced progression to invasive PDAC. All mice showed well to moderately differentiated primary PDACs (Fig. 4*E*) with local invasion and three of five of the animals presented with liver (Fig. 4 *B*, *C*, and *F*), lung (Fig. 4 *D* and *G*), and lymph node metastases (data not shown) similar to mice with expression of mutant TP53^{R172H} (24) or deficiency in TP53 (27, 32). We verified RNAi mediated silencing of TP53 expression by quantitative real-time RT-PCR by using primary tumors of RCASBP(A)-shTP53 and -shControl-infected animals (Fig. S8). Thereby, we demonstrate that RCAS-TVA-mediated spatiotemporal knockdown of gene expression in the pancreas is feasible *in vivo*. In addition, our results confirm previous studies showing that RCASBP(A)-mediated oncogene delivery is capable of modeling human cancer in mice (9, 12, 15, 17, 18). The observed robust and versatile spatiotemporal gene transfer and knockdown makes the system particularly useful to study the role of oncogenes and tumor suppressor genes for tumor initiation and progression (3, 18, 33). It is widely accepted that sporadic human carcinogenesis is caused by sequential accumulation of mutations in oncogenes and tumor suppressor genes in single somatic cells (34). RCAS-mediated oncogene expression or tumor suppressor gene silencing takes place in a limited number of developmentally normal somatic cells with normal microenvironment and, therefore, mimics clonal evolution of sporadic human cancer very closely.

It has been reported that various genes of interest can be simultaneously or sequentially delivered into the same cells of a single mouse line by RCASBP(A) viruses. Therefore, it will be possible to recapitulate multistep carcinogenesis and the cooperation of oncogenes and tumor suppressor genes *in vivo* by using the *LSL-R26$^{Tva-lacZ}$* mouse line (9). The use of RCASBP(A) vectors carrying two or more expression cassettes like an oncogene and a shRNA directed against a tumor suppressor gene, within the same vector will facilitate such studies in the future. Virtually any sequence, cDNA, regulatory RNA, shRNA, or miRNA of <2.5 kb can be expressed by RCASBP(A)-mediated delivery in specific tissue types *in vivo*. Sequences beyond 2.5 kb

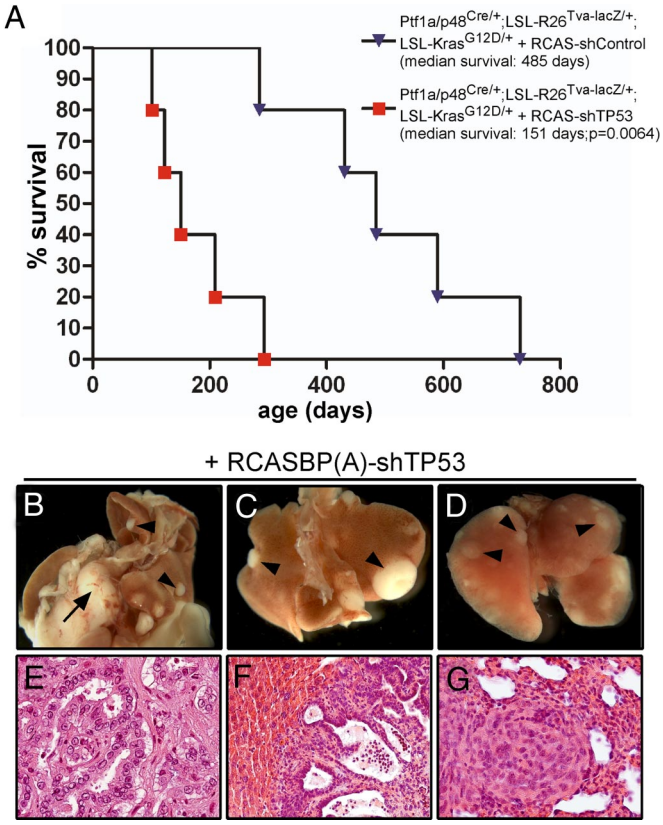

Fig. 4. RCAS-mediated down-regulation of TP53 accelerates PDAC formation in mice with endogenous expression of oncogenic Kras^{G12D} in the pancreas. Three-week-old *Ptf1a/p48$^{Cre/+}$;LSL-R26$^{Tva-lacZ/+}$;LSL-Kras$^{G12D/+}$* mice were infected with RCASBP(A) virus carrying a short hairpin RNA directed against murine TP53 [RCASBP(A)-shTP53] or a control shRNA [RCASBP(A)-shControl] as described in the Materials and Methods section. (*A*) Kaplan–Meier survival curves of *Ptf1a/p48$^{Cre/+}$;LSL-R26$^{Tva-lacZ/+}$;LSL-Kras$^{G12D/+}$* littermates infected with RCASBP(A)-shTP53 (red squares) or RCASBP(A)-shControl (blue triangles) reveal a statistically significant decreased median survival of RCASBP(A)-shTP53-infected mice (151 days), compared with RCASBP(A)-shControl-infected animals (485 days) (P = 0.0064; log-rank test). (*B–D*) Macroscopic view of PDAC (*B*; black arrow), liver metastases (*B* and *C*; black arrowheads) and lung metastases (*D*; black arrowheads) arising in RCASBP(A)-shTP53-infected mice. (*E–G*) H&E-stained paraffin sections of primary PDAC (*E*), liver (*F*), and lung (*G*) metastasis.

cannot be packaged efficiently into RCASBP(A) viruses. However, the new mouse line can be used with other retroviral or lentiviral vectors pseudotyped with envA. Such strategies have been used *in vitro* to deliver expression cassettes beyond 2.5 kb into TVA-positive cells (7).

In summary, we describe the generation of a mouse model for Cre-inducible TVA expression by insertion of a silenced TVA/lacZnls cassette into the ubiquitously expressed *Rosa26* locus. By taking advantage of the increasing number of Cre-expressing mouse lines and Cre expression strategies (35), our model allows Cre-inducible TVA expression and RCASBP(A)-mediated gene transfer in a wide range of different tissue types and cell populations and therefore overcomes major limitations of existing mouse lines that use tissue-specific promoters for transgenic TVA expression (9, 10, 12, 13, 15, 17–19). Thus, our mouse line opens up many possibilities for analysis of gene function in a time-controlled and tissue-specific fashion *in vivo*. Because our model can be easily combined with Cre-loxP-based conditional gene knockout or knockin mouse lines (35, 36), it expands the applications of the RCAS-TVA system substantially. Thus, it is possible to analyze the collaboration of genes of interest in

defined tissues *in vivo* without the need to generate gene targeted lines.

Materials and Methods

Mouse Strains and Tumor Models. *LSL-Kras^{G12D}* (37), *LSL-TP53$^{R172H/+}$* (38), and *Ptf1a/P48$^{Cre/+}$* (22) mice have been described previously. The strains were interbred with the *LSL-R26$^{Tva-lacZ/+}$* line to obtain mice that develop TVA-positive mPanIN lesions and PDAC. The *LSL-R26$^{Tva-lacZ/+}$* strain was also interbred to the general deleter strain *Prm-Cre* (21) (The Jackson Laboratory) to obtain ubiquitous deletion of the LSL cassette. All animal studies were conducted in compliance with European guidelines for the care and use of laboratory animals and were approved by the local authorities.

Virus Preparation and Infection. RCASBP(A) viruses were generated as described by Du *et al.* (18) with minor modifications. In brief, DF-1 cells (American Type Culture Collection) were transfected with 2.5 μg of the respective RCASBP(A) plasmids by using Superfect (Qiagen). After 2 weeks, supernatants were filtered and used to infect DF-1 cells for virus titer determination by limiting dilution or to infect TD-2 or MiaPaCa2 pancreatic cancer cells (39) with stable expression of firefly luciferase and TVA. Infection of 2-day-old mice was done as described by Lewis *et al.* (15). In brief, DF-1 cells transfected with the respective RCASBP(A) vectors were harvested from culture flasks by trypsinization, washed once with DMEM, and 5×10^7 cells in 100 μl of DMEM were injected i.p. Intrapancreatic delivery of DF-1 cells was done as follows. Mice were anesthetized with isoflurane, medetomidine, midazolam, and fentanyl. A small left abdominal incision was made and the spleen was displayed by a gentle pull. In an area adjacent to the spleen, 10^7 DF-1 cells in 30 μl of DMEM were injected into the pancreas by using a microliter syringe with a 27-gauge needle (Hamilton Syringes).

Additional Methods. Descriptions of additional methods are available in *SI Methods* online.

ACKNOWLEDGMENTS. We thank Dr. P. Soriano (Fred Hutchinson Cancer Research Center, Seattle, WA), Dr. N. Proudfoot (University of Oxford, Oxford, U.K.), Dr. P. Bates (University of Pennsylvania, Philadelphia, PA), Dr. S. Orsulic (Harvard Medical School, Boston, MA), Dr. S. Hughes (National Cancer Institute, Frederick, MD), and Dr. K. Rajewski (Harvard Medical School, Boston, MA) for providing plasmids. We thank Dr. T. Jacks (Massachusetts Institute of Technology, Cambridge, MA) for LSL-Kras^{G12D} and TP53^{+} mice; Dr. F. Greten (Technical University of Munich, Germany) for TD-2 cells; and U. Götz, K. Kellnberger, B. Kohnke-Ertl, and M. Werb for excellent technical assistance. This work was supported by Deutsche Krebshilfe (to D.S.).

1. Frese KK, Tuveson DA (2007) Maximizing mouse cancer models. *Nat Rev Cancer* 7:645–658.
2. Fisher GH, *et al.* (1999) Development of a flexible and specific gene delivery system for production of murine tumor models. *Oncogene* 18:5253–5260.
3. Orsulic S (2002) An RCAS-TVA-based approach to designer mouse models. *Mamm Genome* 13:543–547.
4. Du Z, Li Y (2007) RCAS-TVA in the mammary gland: An in vivo oncogene screen and a high fidelity model for breast transformation? *Cell Cycle* 6:823–826.
5. Bates P, Young JA, Varmus HE (1993) A receptor for subgroup A Rous sarcoma virus is related to the low density lipoprotein receptor. *Cell* 74:1043–1051.
6. Young JA, Bates P, Varmus HE (1993) Isolation of a chicken gene that confers susceptibility to infection by subgroup A avian leukosis and sarcoma viruses. *J Virol* 67:1811–1816.
7. Lewis BC, Chinnasamy N, Morgan RA, Varmus HE (2001) Development of an avian leukosis-sarcoma virus subgroup A pseudotyped lentiviral vector. *J Virol* 75:9339–9344.
8. Pinto VB, Prasad S, Yewdell J, Bennink J, Hughes SH (2000) Restricting expression prolongs expression of foreign genes introduced into animals by retroviruses. *J Virol* 74:10202–10206.
9. Orsulic S, *et al.* (2002) Induction of ovarian cancer by defined multiple genetic changes in a mouse model system. *Cancer Cell* 1:53–62.
10. Federspiel MJ, Bates P, Young JA, Varmus HE, Hughes SH (1994) A system for tissue-specific gene targeting: Transgenic mice susceptible to subgroup A avian leukosis virus-based retroviral vectors. *Proc Natl Acad Sci USA* 91:11241–11245.
11. Holland EC, Varmus HE (1998) Basic fibroblast growth factor induces cell migration and proliferation after glia-specific gene transfer in mice. *Proc Natl Acad Sci USA* 95:1218–1223.
12. Holland EC, Hively WP, DePinho RA, Varmus HE (1998) A constitutively active epidermal growth factor receptor cooperates with disruption of G1 cell-cycle arrest pathways to induce glioma-like lesions in mice. *Genes Dev* 12:3675–3685.
13. Dunn KJ, Williams BO, Li Y, Pavan WJ (2000) Neural crest-directed gene transfer demonstrates Wnt1 role in melanocyte expansion and differentiation during mouse development. *Proc Natl Acad Sci USA* 97:10050–10055.
14. Murphy GJ, Leavitt AD (1999) A model for studying megakaryocyte development and biology. *Proc Natl Acad Sci USA* 96:3065–3070.
15. Lewis BC, Klimstra DS, Varmus HE (2003) The c-myc and PyMT oncogenes induce different tumor types in a somatic mouse model for pancreatic cancer. *Genes Dev* 17:3127–3138.
16. Li L, *et al.* (2005) An in vivo model to study osteogenic gene regulation: Targeting an avian retroviral receptor (TVA) to bone with the bone sialoprotein (BSP) promoter. *J Bone Miner Res* 20:1403–1413.
17. Lewis BC, *et al.* (2005) The absence of p53 promotes metastasis in a novel somatic mouse model for hepatocellular carcinoma. *Mol Cell Biol* 25:1228–1237.
18. Du Z, *et al.* (2006) Introduction of oncogenes into mammary glands in vivo with an avian retroviral vector initiates and promotes carcinogenesis in mouse models. *Proc Natl Acad Sci USA* 103:17396–17401.
19. Du YC, Lewis BC, Hanahan D, Varmus H (2007) Assessing tumor progression factors by somatic gene transfer into a mouse model: Bcl-xL promotes islet tumor cell invasion. *PLoS Biol* 5:2255–2269.
20. Soriano P (1999) Generalized lacZ expression with the ROSA26 Cre reporter strain. *Nat Genet* 21:70–71.
21. O'Gorman S, Dagenais NA, Qian M, Marchuk Y (1997) Protamine-Cre recombinase transgenes efficiently recombine target sequences in the male germ line of mice, but not in embryonic stem cells. *Proc Natl Acad Sci USA* 94:14602–14607.
22. Nakhai H, *et al.* (2007) Ptf1a is essential for the differentiation of GABAergic and glycinergic amacrine cells and horizontal cells in the mouse retina. *Development* 134:1151–1160.
23. Hingorani SR, *et al.* (2003) Preinvasive and invasive ductal pancreatic cancer and its early detection in the mouse. *Cancer Cell* 4:437–450.
24. Hingorani SR, *et al.* (2005) Trp53R172H and KrasG12D cooperate to promote chromosomal instability and widely metastatic pancreatic ductal adenocarcinoma in mice. *Cancer Cell* 7:469–483.
25. Schneider G, Siveke JT, Eckel F, Schmid RM (2005) Pancreatic cancer: Basic and clinical aspects. *Gastroenterology* 128:1606–1625.
26. Hezel AF, Kimmelman AC, Stanger BZ, Bardeesy N, Depinho RA (2006) Genetics and biology of pancreatic ductal adenocarcinoma. *Genes Dev* 20:1218–1249.
27. Guerra C, *et al.* (2007) Chronic pancreatitis is essential for induction of pancreatic ductal adenocarcinoma by K-Ras oncogenes in adult mice. *Cancer Cell* 11:291–302.
28. Hruban RH, *et al.* (2006) Pathology of genetically engineered mouse models of pancreatic exocrine cancer: Consensus report and recommendations. *Cancer Res* 66:95–106.
29. Bromberg-White JL, *et al.* (2004) Delivery of short hairpin RNA sequences by using a replication-competent avian retroviral vector. *J Virol* 78:4914–4916.
30. Harpavat S, Cepko CL (2006) RCAS-RNAi: A loss-of-function method for the developing chick retina. *BMC Dev Biol* 6:2.
31. Ventura A, *et al.* (2004) Cre-lox-regulated conditional RNA interference from transgenes. *Proc Natl Acad Sci USA* 101:10380–10385.
32. Bardeesy N, *et al.* (2006) Both p16(Ink4a) and the p19(Arf)-p53 pathway constrain progression of pancreatic adenocarcinoma in the mouse. *Proc Natl Acad Sci USA* 103:5947–5952.
33. Pao W, Klimstra DS, Fisher GH, Varmus HE (2003) Use of avian retroviral vectors to introduce transcriptional regulators into mammalian cells for analyses of tumor maintenance. *Proc Natl Acad Sci USA* 100:8764–8769.
34. Fearon ER, Vogelstein B (1990) A genetic model for colorectal tumorigenesis. *Cell* 61:759–767.
35. Feil R (2007) Conditional somatic mutagenesis in the mouse using site-specific recombinases. *Handb Exp Pharmacol* (178):3–28.
36. Branda CS, Dymecki SM (2004) Talking about a revolution: The impact of site-specific recombinases on genetic analyses in mice. *Dev Cell* 6:7–28.
37. Jackson EL, *et al.* (2001) Analysis of lung tumor initiation and progression using conditional expression of oncogenic K-ras. *Genes Dev* 15:3243–3248.
38. Olive KP, *et al.* (2004) Mutant p53 gain of function in two mouse models of Li-Fraumeni syndrome. *Cell* 119:847–860.
39. Saur D, *et al.* (2005) CXCR4 expression increases liver and lung metastasis in a mouse model of pancreatic cancer. *Gastroenterology* 129:1237–1250.